Macromolecular Research, Vol. 15, No. 1, pp 65-73 (2007)

Preparation of a Porous Chitosan/Fibroin-Hydroxyapatite Composite Matrix for Tissue Engineering

Hong Sung Kim*, Jong Tae Kim, and Young Jin Jung

Department of Biomaterials Engineering, College of Natural Resources & Life Science / Joint Research Center of PNU-Fraunhofer IGB, Pusan National University, Miryang 627-706, Korea

Su Chak Ryu

Department of Nanomaterials, College of Nano Science and Technology, Pusan National University, Miryang 627-706, Korea

Hong Joo Son and Yong Gyun Kim

Department of Life Science & Environmental Biochemistry, College of Natural Resources & Life Science, Pusan National University, Miryang 627-706, Korea

Received November 9, 2006; Revised December 20, 2006

Abstract: Chitosan, fibroin, and hydroxyapatite are natural biopolymers and bioceramics that are biocompatible, biodegradable, and resorbable for biomedical applications. The highly porous, chitosan-based, bioceramic hybrid composite, chitosan/fibroin-hydroxyapatite composite, was prepared by a novel method using thermally induced phase separation. The composite had a porosity of more than 94% and exhibited two continuous and different morphologies: an irregularly isotropic pore structure on the surface and a regularly anisotropic multilayered structure in the interior. In addition, the composite was composed of an interconnected open pore structure with a pore size below a few hundred microns. The chemical composition, pore morphology, microstructure, fluid absorptivity, protein permeability, and mechanical strength were investigated according to the composition rate of bioceramics to biopolymers for use in tissue engineering. The incorporation of hydroxyapatite improved the fluid absorptivity, protein permeability, and tenacity of the composite while maintaining high porosity and a suitable microstructure.

Keywords: chitosan, fibroin, hydroxyapatite, composite, porous matrix, pore morphology.

Introduction

Tissue engineering has recently emerged as a potential alternative to tissue transplantation. A biodegradable porous material in tissue engineering serves as a temporary scaffold inserted into the defective sites to support and stimulate tissue regeneration while it gradually degrades and is replaced by new tissue.[1-3] A desirable material for use in the scaffold is a resorbable biomimetic material that induces and promotes new tissue formation at a required site. Both biodegradable polymers and bioactive ceramics have been developed for various tissue engineering applications. The development of new biomaterials has recently focused on the design of biomimetic structural materials that are ubiquitous in nature, which are mainly composed of different constituents; i.e., a hybrid of inorganic crystallites as reinforcing fillers with polymers as matrix. Many biodegradable synthetic polymers including polylactide have been used to develop a biocompatible scaffold.[4-6] These polymer scaffolds have some advantages as they are biodegradable, strong and easy to process into desired shapes. However, they also have several obvious weaknesses, such as hydrophobicity and acidic degradation products which are released continuously *in vivo* and invoke a chronic immune response.[7,8] Besides, their hydrophobic surfaces hinder a cell adhesion and growth in a three-dimensional structure. Numerous efforts have been directed toward finding alternative materials, especially including the study of naturally occurring polymers.[9,10]

Of the known natural biopolymers considered for biomedical applications, one greatly attractive material is chitosan, which is a polyheterosaccharide comprised of glucosamine and *N*-acetylglucosamine units linked by 1-4 glucosidic bonds. Much attention has been paid to chitosan-based biomedical materials because of their unique properties such as biodegradability, nontoxicity, anti-bacterial effect and biocompatibility.[11-13] The chitosan structurally resembles glycosamino-

*Corresponding Author. E-mail: khs@pusan.ac.kr

glycans, consisting of a long-linear chain and repeating disaccharide units. Glycosaminoglycans are branched to a protein core forming proteoglycans, which are thought to play a key role in modulating cell settlement, differentiation, and viable function.[14,15] Chitosan, a natural cationic polymer, has a hydrophilic surface promoting cell adhesion, proliferation, and differentiation, and evokes a minimal foreign body reaction on implantation in comparison with synthetic polymers.[16,17] In this study, we have chosen chitosan to formulate biomatrix as well to act as a suitable binder for bioceramics due to its biocompatibility, resorbability, hemostasis, antiinfectivity, plasticity, and adhesiveness.

Silk fibroin have recently been considered for biomedical materials with a wide variety of applications ranging from skin and vascular grafts to substrates for mammalian cell culture. Fibroin is a linear polypeptide that is composed of 17 amino acids, and has a β-sheet structure because its main components are simple nonpolar ones such as alanine and glycine.[18] It has been reported that silk fibroin acts as an enzyme immobilization matrix with good mechanical properties, and has blood compatibility and good dissolved oxygen permeability in the wet state.[19] There have been reports on silk fibroin/chitosan blend membranes with good mechanical properties forming an interpenetrating polymer network.[20-22]

The extracellular matrices of hard tissue are composed of complex organic-inorganic composite materials, the inorganic crystalline phase consisting primarily of hydroxyapatite, and the organic constituent consisting mainly of collagen and ground substances including glycosaminoglycans, proteoglycans and glycoproteins. The biomimetic approaches on the structure and composition; i.e., the composite of chitosan, fibroin and hydroxyapatite, may provide the possibility of creating more developed biomaterials. The key to successful implantation of the biomaterials is to provide the repair site with sufficient osteogenic progenitor cells and to insure osteoblastic differentiation and optimal secretory activity. Those scaffolding materials should not be isolated by fibroblast and should adhere to the host tissue due to bioactivity; thus, they should be assimilated with the surrounding bone.[23] Hydroxyapatite, a major inorganic component of natural bone, has been used extensively for biomedical implant applications and bone regeneration due to its bioactive, biodegradable and osteoconductive properties.[24,25] It is known also to be biocompatible, non-toxic, non-inflammatory, and non-immunogenic, having the ability to form a direct chemical bond with surrounding hard tissues. Despite their favorable biological properties, hydroxyapatite blocks are inherently brittle and have low biodegradation rates, which severely limits their clinical use. For the treatment of periodontal osseous defects and alveolar ridge augmentation, hydroxyapatite has been used mainly in the form of a particulate because of its easy fabrication, handling and close surface contact with the surrounding tissue. However, the particulate hydroxyapatite is often unstable when the particles are mixed with saline or a patient's blood; hence, it migrates from the implanted site into surrounding tissues, causing damage to healthy tissue.[26,27] The viscoelastic nature of polymer prevents a migration of the particulate into the surrounding tissue upon post-implantation. Therefore, it is desirable to develop a hybrid material with favorable properties of chitosan-based biopolymer and hydroxyapatite for hard tissue regeneration. When the chitosan-based hydroxyapatite composite implanted in a body as a tissue scaffold, relatively fast degradation of chitosan makes room for the growth of new tissue and increases the opportunity to assimilate hydroxyapatite with the host bone.[28] Moreover, it has been reported that chitosan can promote nucleation and growth of natural apatite crystals as well.[29]

For cell transplantation and tissue engineering, a scaffold must be fabricated into a three-dimensional structure with a high porosity and an appropriate pore size. Various techniques have been utilized to prepare such highly porous scaffolds.[30-32] Recently, a new procedure for preparing porous matrix from a polymer solution by thermally inducing phase separation (TIPS) and subsequent sublimation of the solvent has generated considerable interest. In this procedure, two phases - a polymer-rich phase and a solvent-rich phase - are formed by cooling down the polymer solution to induce liquid-liquid or solid-liquid phase separation. The solvent is then removed by solvent extraction or sublimation *in vacuo* to form pores.[4,33,34]

Here, we present a novel way to prepare composite matrices of chitosan/fibroin and hydroxyapatite with high porosity by a TIPS. The chemical composition, microstructure, pore morphology, fluid absorptivity, protein permeability, and tenacity were systematically investigated according to the rate of hydroxyapatite in the composite.

Experimental

Materials. Chitosan was obtained from Taehoon-Bio, Korea, and purified as follows. The chitosan flake was dissolved in a 2 wt% aqueous acetic acid solution until a homogeneous 1 wt% chitosan solution was obtained. This solution was neutralized with a 2 wt% sodium hydroxide solution to precipitate chitosan. Next, the latter was washed with deionized water and ethanol, and then vacuum-dried. The purified chitosan has a degree of deacetylation of 97% and a weight averaged molecular weight of 400,000.

Raw silk produced by *Bombyx mori* silkworms was degummed and dissolved in a mixed solvent of $CaCl_2$, H_2O, and ethanol. The fibroin aquous solution was dialyzed in flowing water for 7 days.

Hydroxyapatite (HAP) powder, with a stoichiometric ratio of Ca to P (=1.55), was obtained from HAP Tech Inc., Korea. To reduce average particle diameter, an agateball mill was used. The purity of the powder was confirmed by X-ray diffraction and infrared spectrum. The HAP powder was dis-

persed in an aquous acidic solution and ultrasonicated, resulting in an ultimate average particle size of approximately 2 μm measured using a Zeta potential particle analyzer.

The rest of the chemicals utilized in this experiment were used as a guarantied reagent grade without any further purification: bovine serum albumin-fluorescein isothiocyanate conjugate (FITC-BSA), acetic acid, calcium chloride hexahydrate, ethanol, and sodium hydroxide from Sigma-Aldrich Co., USA.

Fabrication of Composites. The chitosan/fibroin biopolymer blend (CFB) - hydroxyapatite composite matrices were prepared by TIPS and subsequent sublimation of the solvent. HAP powder was dispersed in 2 wt% acetic acid solution with desired concentration. The solution was stirred and treated by ultrasonication for 20 min to disperse HAP particles uniformly. Next, 2 wt% chitosan was dissolved in the HAP dispersed solution at room temperature and stirred for 5 hrs to create a homogeneous mixed solution. The HAP content of each specimen was scaled according to the CFB/HAP weight ratios of 100/0, 90/10, 80/20, 70/30, 60/40, 50/50, 40/60, and 30/70, which were listed in Table I. The fibroin aquous solution was blended in the HAP-dispersed chitosan solution with the constant weight ratio of fibroin to chitosan (=0.2). This ratio was ascertained as an optimum condition on some properties of CFB, e.g., relatively lower crystallinity and higher water-absorptivity, for a biomedical matrix as in our previous papers.[35] The CFB-HAP composite solution was vigorously stirred, forming a mechanically induced liquid-gas colloid (foamy solution). The foamy composite solution was put into a PET mold and rapidly transferred to a freezer at -98 °C to solidify the solvent and induce liquid-liquid or solid-liquid phase separation. The solidified mixture was maintained at that temperature for 24 hrs, transfered into a freeze-drying vessel and lyophilized until dried. The dried composites were again vacuum-dried at 0.5 mmHg and 60 °C for at least 2 days in order to eliminate the remaining solvents, especially acetic acid, and to form highly porous matrices with a thickness of approximately 4 mm. These matrices were stored in a desiccator until characterization. The composition of the composite matrix was determined by the rate of HAP content to CFB as shown in Table I.

Table I. Densities and Porosities of CFB/HAP Composites

CFB/HAP Composition (wt/wt)	Fibroin Conc. in CFB (wt%)	Density (g/cm^3)	Porosity (%)
100/0	20	0.81	98.0
90/10	20	0.89	98.2
80/20	20	0.93	97.6
70/30	20	0.95	97.3
60/40	20	0.98	96.5
50/50	20	1.03	95.7
40/60	20	1.11	95.4
30/70	20	1.20	94.4

*CFB: Chitosan/fibroin biopolymer blend.

***In Vitro* Tests.** In order to investigate the fluid absorptivity and stability of CFB-HAP composite matrices, the *in vitro* experiment was conducted in a simulated body fluid (SBF). The SBF solution was prepared by dissolving reagent-grade NaCl, $NaHCO_3$, KCl, $K_2HPO_4 \cdot 3H_2O$, $MgCl_2 \cdot 6H_2O$, $CaCl_2$, and Na_2SO_4 in deionized water, whose ionic concentrations are shown in Table II. The solution was buffered at pH 7.4 with tris(hydroxymethyl) aminomethane and 1 M hydrochloric acid at 36.5 °C.

The weight of dried specimens was marked as W_0 and the specimens were immersed in SBF for a desired times at 37 °C. After being immersed, the specimens were removed from SBF, gently rinsed with deionized water 5 times, cleaned with filter paper to get rid of liquid on the surface, and then weighed and marked as W_1. After being dried, the specimens were weighed again and noted as W_2. The SBF absorptivity was determined by the equation $(W_1 - W_0)/W_0$, and the rate of weight loss by the equation $(W_0 - W_2)/W_0$.

Protein permeability was performed by using a side-by-side diffusion cell which had 50 mm^2 diffusion area. FITC-BSA was used as a model nutriment. The donor cell installed specimen was filled with 3 mL of SBF in which FITC-BSA was dissolved at a concentration of 1 mg/mL and receptor cell on the other side was filled with 3 mL of SBF only. This diffusion cell set was placed in an incubator at 37 °C with stirring. The whole SBF in the receptor cell was extracted each desired time, and then was measured the absorbency of the FITC excitation wavenumber at 495 nm by utilizing a UV spectrophotometer.

Instruments and Measurements. Chemical analysis of the composite matrix was carried out by a Fourier transform infrared spectrophotometer (FTIR; Perkin Elmer Spectrum GX, USA) within a range of 4000 to 400 cm^{-1} at 0.3 cm^{-1} resolution. The porous morphologies of the composite matrix,

Table II. Ionic Concentrations of SBF in Comparison with Those of Human Blood Plasma

	Concentration (mM)							
	Na^+	K^+	Ca^{2+}	Mg^{2+}	HCO_3^-	Cl^-	HPO_4^{2-}	SO_4^{2-}
Blood Plasma	142.0	5.0	2.5	1.5	27.0	103.0	1.0	0.5
SBF	142.0	5.0	2.5	1.5	27.0	125.0	1.0	0.5

sputter-coated with platinum in a Hitachi E1010 ion sputter, were examined by scanning electron microscopy (SEM; Hitachi S-3500N, Japan) at 15 kV. The porosity and density was determined from variation of volume by compression of 25 kg/mm^2 using a presser and precision tile mold (Carver 3393, USA). Crystallographic studies were carried out with X-ray diffractometer (XRD; Rigaku Dmax 2000 V, Japan) using monochromatic CuKα radiation at 50 kV and 30 mA. The tenacity was tested using universal testing machine (United SSTM-1, USA) with 5 kg_f load cells.

Results and Discussion

Chemical Composition by FTIR. As shown in FTIR spectra of Figure 1, the absorption bands at 1643, 1598, 1243, and 1072 cm^{-1} are the characteristic bands of amide I, amide II, amide III, and -C-O- vibration of glucosamine. The absorption bands at 1634 and 650 cm^{-1} are the characteristic bands of amide I and amide V vibration of fibroin, while 1542 (amide II) and 1241 cm^{-1} (amide III) bands of fibroin were buried in relatively strong amide bands of glucosamine. The two bands at 631 and 3570 cm^{-1} belong to the vibration of hydroxyl. The bands at 1045 and 1091 cm^{-1} are the characteristic bands of phosphate stretching vibration, while the bands at 603 and 570 cm^{-1} are due to phosphate bending vibration. The intensity of the vibration at 1072 cm^{-1} relatively decreases with increasing HAP rate, and was gradually buried in phosphate vibration at 1045 cm^{-1}. The characteristic bands of all components; that is, chitosan, fibroin, and HAP, were observed, and were shown a variation of the absorption intensity depending on the relative content of the component. The amide carbonyl absorption at 1634 cm^{-1} was assigned to the β-sheet structure of fibroin in CFB composite (100/0 rate), which did not contain HAP.[20,36] With an increasing HAP rate, this absorption was shifted to a higher wavenumber and was gradually merged with amide carbonyl absorption of glucosamine at 1643 cm^{-1}. Therefore, it could be suggested that the fibroin conformation was a β-sheet structure in the CFB composite, but changed to a random coil structure in the composite with HAP.

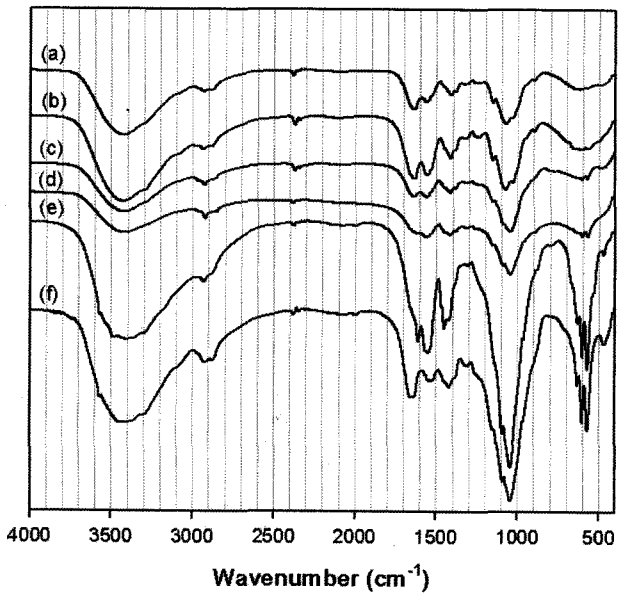

Figure 1. FTIR spectra of chitosan/fibroin-hydroxyapatite composites with biopolymers/HAP weight ratios of (a) 100/0, (b) 90/10, (c) 70/30, (d) 50/50, (e) 30/70, and (f) the 50/50 composite immersed in SBF for 2 weeks.

Chitosan is characterized by forming chitosan-metal complexes in which metal ions coordinate with amino groups of chitosan.[37] During the composite process, chitosan encloses the HAP particulate inside the polymer. It has been reported that the *c-axis* of HAP crystals tends to align along the chitosan chains.[38] After being compounded with HAP, the glucosamine amide II adsorption at 1598 cm^{-1} in CFB composite shifted to a lower wavenumber at 1567 cm^{-1}; and the glucosamine amide III adsorption at 1243 cm^{-1} disappeared. This suggests that an interaction takes place between CFB and HAP, including hydrogen bonds of glucosamine amino with HAP hydroxy and the chelation of glucosamine amino with Ca^{2+}.

In 50/50 composite immersed in SBF for 2 weeks as shown in Figure 1(f), the phosphate adsorption at 1045 cm^{-1} remained unchanged with strong intensity, but the glucosamine amide I adsoption shifted to a distinctly higher wavenumber of 1659 cm^{-1}. These changes suggest that the HAP received no noticeable influence in SBF within a given period, but the positively charged amino groups of chitosan formed an ionic complex with the negatively charged components, such as phosphates of HAP and/or various kinds of dissociated salts absorbed from SBF solution.[39]

Morphology by SEM. High porosity composite matrices have been prepared by a TIPS and subsequent sublimation of the solvent. With increasing HAP content, the density increases and the porosity decreases inversely as listed in Table I. The porosities of the composite matrices were determined to be at least 94%, which was considered to be beneficial for cell ingrowth and survival. Scaffolds for tissue engineering must have a highly porous and interconnected pore structure to ensure a biological environment conducive to cell attachment and proliferation, in addition to providing the mass transport of nutrients, metabolites, and soluble signals.[30,40]

Figures 2 and 3 show surfaces of the composite matrices and the magnified surfaces of the pore wall. Freeze drying of the phase-separated CFB/HAP/solvent mixtures produced a porous matrix with a continuous structure of interconnected pores and the CFB/HAP composite skeleton composed of thin polymeric leaflets (Figure 2(D)). The irregular pores ranged from several microns up to a few hundred microns. The HAP particulates ranging from 0.5 to 2 μm in size were well dispersed in the pore walls, presumably due to the high viscosity of the polymeric solution. SEM observation demo-

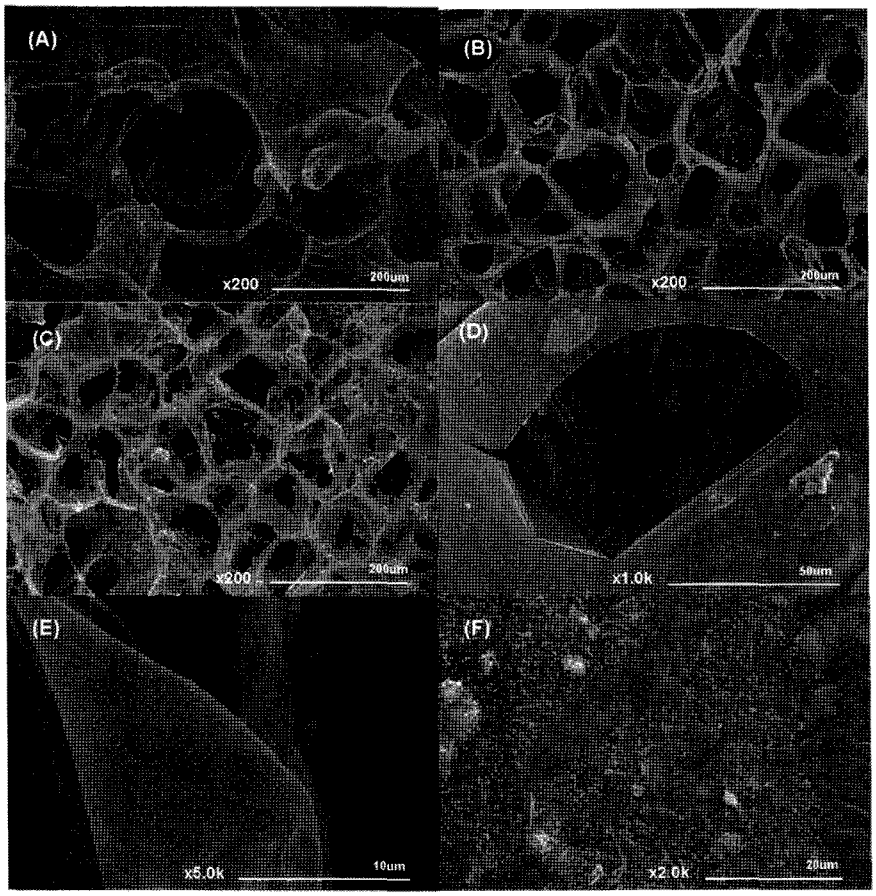

Figure 2. SEM images from the surfaces of chitosan/fibroin-hydroxyapatite composite with biopolymers/HAP weight ratios of (A) 100/0, (B) 70/30, (C) 50/50 at a magnification of × 200, (D) 50/50 at × 1000, (E) 50/50 at × 5000, and (F) 30/70 at × 2000.

strates that the micropore structure of the composite matrix changes considerably with the HAP content (Figures 2(A)-(C)). Most of the HAP particulates that bonded to a polymeric matrix were on the surfaces of the thin solid walls of the pores. When the HAP content is lower, the HAP particulate acting as a filling phase are dispersed uniformly in the continuous polymeric phase (Figure 2(E)). However, with the increase of HAP content, the polymeric phase is insufficient to enclose the HAP particulates and merely acts as a glue to bond these particulates together, resulting in partial agglomerates (Figures 2(F) and 3(D)). The matrix prepared from the 30/70 composite was relatively stiff and brittle.

On the other hand, as shown in Figure 3, the composite matrix also has a highly anisotropic multilayered morphology with internal apertures. This multilayered structure is a characteristic morphology formed by phase separation of a polymeric solution. When the temperature of the polymeric solution is lower than the freezing point of the solvent, the crystallization of the solvent takes place, and the polymer phase is expelled from the crystallization front. A continuous polymer-rich phase is formed by aggregation of polymers expelled from solvent crystals. After the solvent crystals have been sublimated, the porous matrix forms with multi-channel apertures similar to a morphology of solvent crystals. In the composite matrix, the channels were parallel to the solidified direction of the aquous acetic solution. Each channel was divided by repeating partitions with uniform spacing which varied depending on the cooling rate and the polymer concentration. The freezing point of the acetic solution was about -13 °C estimated by a molar depression constant and molarity of solute in the solution. The HAP content did not affect the solvent crystallization enough to alter the pore structure morphology significantly (Figures 3(A)-(C)).

The temperature gradient along the heat transfer direction in the freezing matrix takes place in a lyophilizing vessel during the vacuum process, and dissolves solvent crystals on the outside of the matrix before sublimation, resulting in a collapse of the phase separation in the surface domain. This may have led to the simultaneous formation of two different morphologies; namely, irregularly isotropic pore structure in the matrix surface and regularly anisotropic multilayered structure in the interior of the matrix (Figure 3(E)). The composite matrix shrinked during freeze drying, which is attributed to the rearragement of polymer chains in the amor-

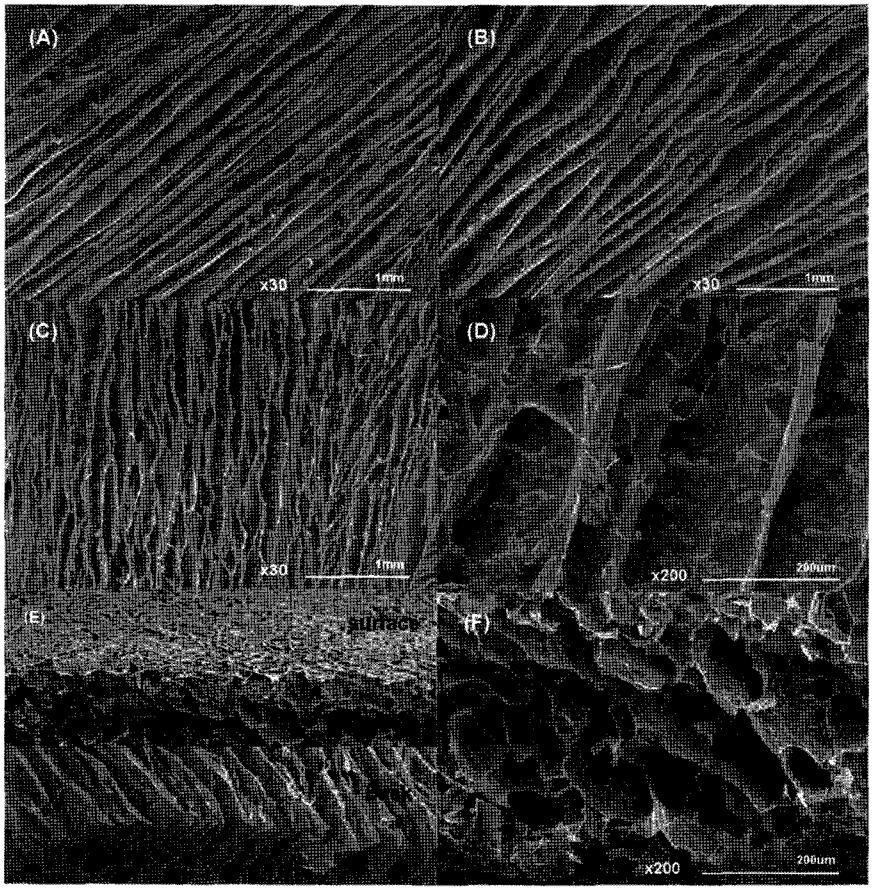

Figure 3. SEM images taken from the inside of the composite with biopolymers/HAP weight ratios of (A) 100/0, (B) 80/20, (C) 50/50 at a magnification of ×30, (D) 70/30 at ×200, and (E) comparison images of the surface and the back in 40/60 composite toward the sublimated direction of the solvent; the upper image is the surface at ×70 and the lower image is the back at ×30, and (F) lateral section at ×200.

phous phase occuring predominantly by quick freezing. This means the formation of a crystalline phase which governs mechanical properties of the composite.

Microstructure by XRD. Figures 4(a)-(f) shows the X-ray diffraction patterns for the composite matrices with weight ratios of HAP. Many sharp diffractions correspond to (100), (002), (102), (210), (211), (112), (300), (202), and (310) reflections of HAP crystal respectively, and are of a typical apatite crystal structure. The sharp diffraction prove that HAP is composed of well-developed crystals. The undifferentiated broad diffraction peaks of the CFB composite of around $2\theta = 20°$ seem to be diffused by an overlaping (130) reflection of chitosan on a (201) reflection attributed to the β-structure of fibroin.

The XRD patterns of the composites according to HAP content made little difference with respect to the diffraction angle except that diffraction intensities of HAP were conspicuously strengthened. This means that the presence of chitosan did not induce any structural deformation of HAP. However, the XRD pattern around the characteristic region near $2\theta=32°$ for low content of HAP revealed broad peaks with poor crystallinity. It is evident that increasing the HAP content decreased the crystallinity of CFB and increased the crystallinity of HAP.

Figure 4(g) shows XRD diffractogram for the 70/30 composite immersed in SBF for 2 weeks. It can be observed that the specific diffraction of CFB around $2\theta=20°$ almost disappeared, whereas the intensity of the specific diffractions for HAP were clearly strengthened after immersing. The biopolymers in the composite swelled in SBF, and reduced partially with dissolution or degradation. Furthermore, its crystalline phase dissolved, which made the diffraction for CFB almost undetectable. On the other hand, the immersing process caused more HAP particles to be expose and thus induced more HAP crystals to deposit. A similar phenomenon in chitosan/tricalcium phosphate composite was reported by Y. Zhang *et al.*[41]

***In Vitro* Absorptivity and Stability.** The *in vitro* absorptivity and leaching stability of the composite matrix in SBF solution (pH 7.4) were quantitatively measured according to immersing time and graphically represented in Figure 5(A). The 80/20 composite swelled with an absorption rate of

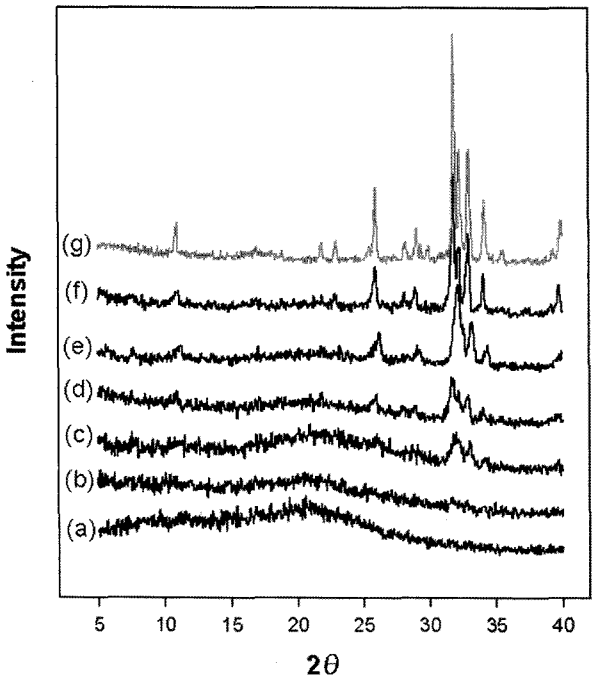

Figure 4. XRD patterns of chitosan/fibroin-hydroxyapatite composites with biopolymers/HAP weight ratios of (a) 100/0, (b) 90/10, (c) 80/20, (d) 70/30, (e) 60/40, and (f) 50/50, and (g) the 70/30 composite immersed in SBF for 2 weeks.

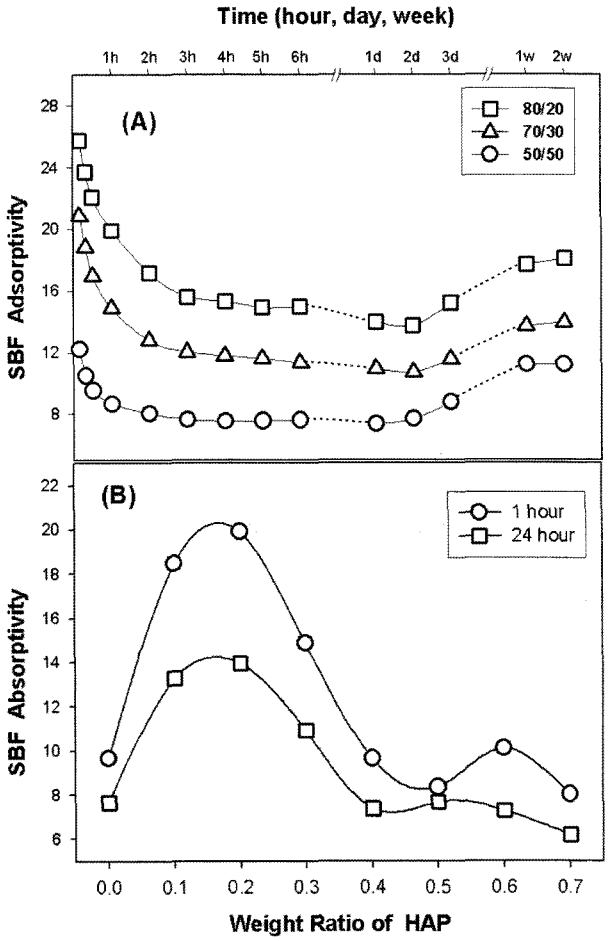

Figure 5. The SBF absorptivity as a function of (A) immersing time and (B) weight rate of HAP in the composite.

about 25 in a few minutes and underwent a minor swelling thereafter at a rapidly reduced rate. After approximately 3 hrs, the absorption rate was nearly constant. For all specimens, a similar trend was observed. Most natural biopolymers swell readily in biological fluids because of an attractive interaction of their hydrophilic groups with ionic solutes. This initial swelling of the composite matrix may be due to the absorption of ionic solutes in SBF by complex formation. The disconnection of the intermolecular bond of CFB chains by ionic solutes leads to more flexible chains, which can hold more water.

However, the absorption rate again began to increase slowly after approximately 2 days, and was kept stable after 1 week. The rate of weight loss was about 3 wt% after 1 week, and remained intact for 4 weeks. The weight loss seems to be ascribed to dissolution and/or degradation of biopolymers involving the protonation of amino groups of glucosamine. There are several parameters affecting the adsorption rate, including the hydrophilicity, crystallinity, and pore structure. The equilibrium between the content of hydrophilic polymers and the crystallinity decides the absorptivity in case where a dissolution and transformation of the microstructure occur in the solution. Despite some dissolution, this second increment is attributed to the decrease in the polymeric crystalline phase in swelling conditions as described in the XRD result.

The SBF absorptivity to rate of HAP is shown in Figure 5 (B). Up to a 0.2 rate (80/20 composite), the absorptivity was increased due to a lowering of crystallinity and intermolecular interaction in the amorphous phase. However, the absorptivity again decreased due to the lowering of the hydrous polymer portion and a lowering of porosity as shown in Figure 2 and Table I because the pore was filled and covered with agglutinated HAP crystals.

Such initial swelling is desirable and the resultant increase in pore size was reported to facilitate cell attachment and growth in a three-dimensional structure.[42] The swelling behavior and leaching stability of substrate are critical for their practical use in tissue engineering.

Protein Permeability. Recent research demonstrated that cell adhesion and survival could be modulated by continuous provision of extracellular matrix components and serum proteins on the substrate.[43] The protein permeation is an important factor in evaluating the substrate for tissue engineering. For evaluating the protein permeability of the composite matrix, we used a coupled diffusion cell device and FITC-BSA as a model protein. As shown in Figure 6, the protein permeation was increased almost linearly according to lapse of time.

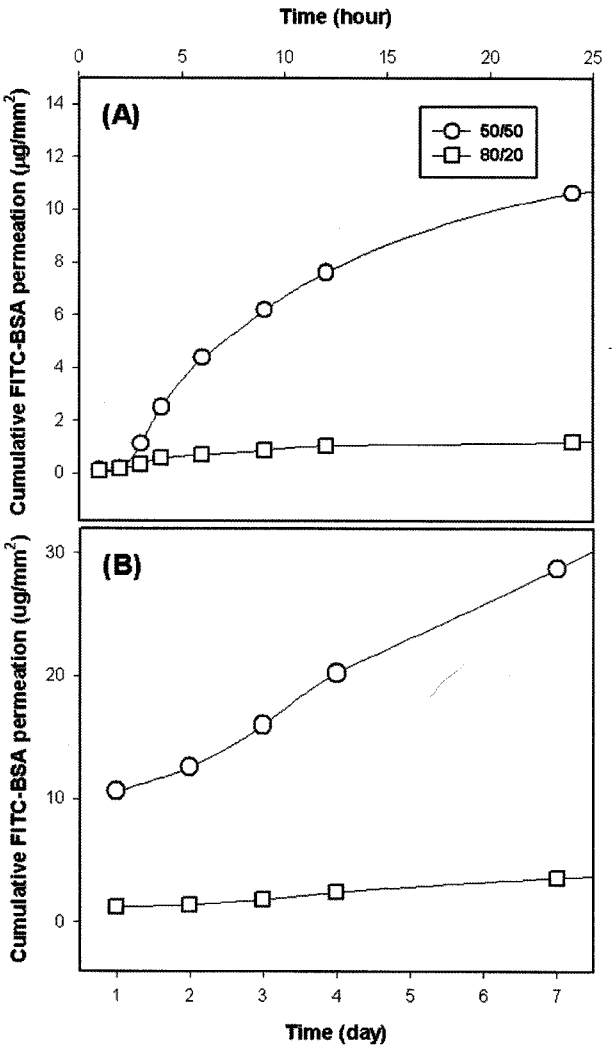

Figure 6. The protein permeability as a function of elapsed time.

The proper content of the HAP (50/50 composite) greatly enhanced permeability in comparison with other HAP rates. This is especially so with an 80/20 composite, which showed the highest SBF absorptivity. This 50/50 composite had the lowest absorptivity, an amorphous polymeric phase, and an agglutinate of well-developed HAP crystals as in the above analyses. These results suggested that the protein permeation of the composite matrix was obstructed instead by its absorptiveness and influenced effectively by the pore structure. In addition, the permeability could be regulated by HAP content.

Mechanical Strength. The composite matrix must have sufficient porosity for cell growth, but also must maintain enough mechanical strength to support the frame during tissue regeneration. The tenacity of the composite matrices were compared depending on HAP content and shown in Figure 7. The tenacity was gradually increased to a 60/40 ratio according to HAP content, but was remarkably reduced at 50/50.

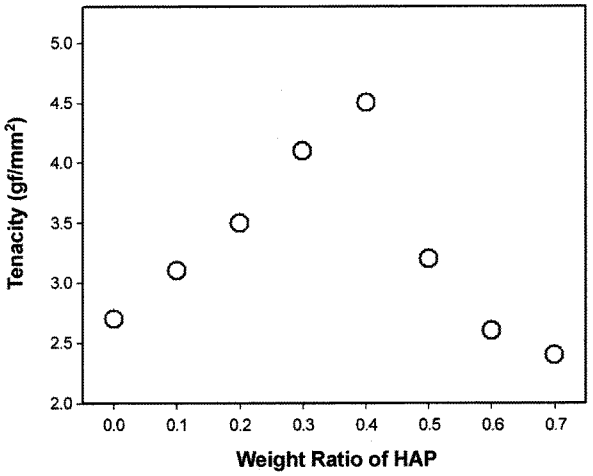

Figure 7. The tenacity as a function of the weight rate of HAP in the composite.

In general, the proper stress transfer occurring between the reinforcement and the matrix governs the mechanical characteristics of filled polymers.[44] These data demonstrate the positive synergetic effects of HAP filling in enhancing the mechanical performance of the composite matrix with less than a 50/50 ratio of HAP to polymers, and it also demostrate the insufficience of the polymeric phase in maintaining the mechanical performance in the case of an excessive HAP content of more than a 50/50 ratio.

Conclusions

In this work, the chitosan/fibroin-hydroxyapatite composite matrix for tissue engineering was fabricated by a TIPS. We developed a novel method for preparing the composite matrix to create a highly porous structure with two continuous and different morphologies of irregularly isotropic pore structure in the matrix surface and a regularly anisotropic multilayered structure in the interior of the matrix. In the composite matrix, porosity as high as 94% was achieved, and the interconnected open pore structure with a pore size ranging from several microns to a few hundred microns was formed.

The variation of material properties including chemical composition, pore morphology, microstructure, SBF absorptivity, protein permeability, and tenacity were investigated by varying the weight ratio of HAP to CFB. The incorporation of HAP improved the SBF absorptivity, protein permeability, and mechanical strength of the composite while maintaining high porosity and a suitable microstructure.

A more detailed study of biological properties including enzyme-degradation is underway and will be reported separately together with tissue formation in this composite matrix.

Acknowledgements. This work was supported by 2006 Joint Research Center of PNU- Fraunhofer IGB Grant of

Pusan National University.

References

(1) J. L. Drury and D. J. Mooney, *Biomaterials*, **24**, 4337 (2003).
(2) G. Khang, M. S. Kim, S. H. Cho, I. Lee, J. M. Rhee, and H. B. Lee, *Tissue Engineering and Regenerative Medicine*, **1**, 9 (2004).
(3) A. Steinbuchel and R. H. Marchessault, *Biopolymers for Medical and Pharmaceutical Applications*, Wiley-VCH, Weinheim, 2005.
(4) F. J. Hua, T. G. Park, and D. S. Lee, *Polymer*, **44**, 1911 (2003).
(5) J. Guan, K. L. Fujimoto, M. S. Sacks, and W. R. Wagner, *Biomaterials*, **26**, 3961 (2005).
(6) H. -J. Jin, M. -O. Hwang, J. S. Yoon, K. H. Lee, I. -J. Chin, and M. -N. Kim, *Macromol. Res.*, **13**, 73 (2005).
(7) A. U. Daniels, K. P. Andriano, W. P. Smutz, M. K. O. Chang, and J. Heller, *J. Appl. Biomater.*, **5**, 51 (1994).
(8) L. Li, S. Ding, and C. Zhou, *J. Appl. Polym. Sci.*, **91**, 274 (2004).
(9) D. L. Ellis and I. V. Yannas, *Biomaterials*, **17**, 291 (1996).
(10) F. Zhao, Y. Yin, W. W. Lu, J. C. Leong, W. Zhang, J. Zhang, M. Zhang, and K. Yao, *Biomaterials*, **23**, 3227 (2002).
(11) A. Lahiji, A. Sohrabi, D. S. Hungerford, and C. G. Frondoza, *J. Biomed. Mater. Res.*, **51**, 586 (2000).
(12) P. V. Vandevord, H. W. T. Matthew, S. P. Desilva, L. Mayton, B. Wu, and P. H. Wooley, *J. Biomed. Mater. Res.*, **58**, 585 (2002).
(13) C. H. Kim, H. -S. Park, Y. J. Gin, Y. Son, S. -H. Lim, Y. J. Choi, K. -S. Park, and C. W. Park, *Macromol. Res.*, **12**, 367 (2004).
(14) H. Nishikawa, A. Ueno, S. Nishikawa, J. Kido, M. Ohishi, H. Inoue, and T. Nagata, *J. Endodontics*, **26**, 169 (2000).
(15) S. Szuchet, K. Watanabe, and Y. Yamaguchi, *Int. J. Dev. Neurosci.*, **18**, 705 (2000).
(16) J. K. Suh and H. W. Matthew, *Biomaterials*, **21**, 2589 (2000).
(17) M. Ishihara, K. Nakanishi, K. Ono, M. Sato, M. Kikuchi, Y. Saito, H. Yura, T. Matsui, H. Hattori, M. Uenoyama, and A. Kurita, *Biomaterials*, **23**, 833 (2002).
(18) G. Freddi, P. Monti, M. Nagura, Y. Gotoh, and M. Tsukada, *J. Polym. Sci.; Part B: Polym. Phys.*, **35**, 841 (1997).
(19) N. Minoura, S. Aiba, Y. Gotoh, M. Tsukada, and Y. Imai, *J. Biomed. Mat. Res.*, **29**, 1215 (1995).
(20) X. Chen, W. Li, and T. Yu, *J. Polym. Sci.; Part B: Polym. Phys.*, **35**, 2293 (1997).
(21) H. Kweon, H. C. Ha, I. C. Um, and Y. H. Park, *J. Appl. Polym. Sci.*, **80**, 928 (2001).
(22) G. D. Kang, K. H. Lee, C. S. Ki, J. H. Nahm, and Y. H. Park, *Macromol. Res.*, **12**, 534 (2004).
(23) T. Kokubo, H. Kim, and M. Kawashita, *Biomaterials*, **24**, 2161 (2003).
(24) J. M. Gomez-Vega, E. Saiz, A. P. Tomsia, G. W. Marshall, and S. J. Marshall, *Biomaterials*, **21**, 105 (2000).
(25) V. M. Rusu, C. Ng, M. Wilke, B. Tiersch, P. Fratzl, and M. G. Peter, *Biomaterials*, **26**, 5414 (2005).
(26) Y. Miyamoto, K. Ishikawa, M. Takechi, T. Toh, T. Yuasa, M. Nagayama, and K. Suzuki, *Biomaterials*, **19**, 707 (1998).
(27) R. Murugan and S. Ramakrishna, *Biomaterials*, **25**, 3829 (2004).
(28) C. Zahraoui and P. Sharrock, *Bone*, **25**, 63 (1999).
(29) R. A. A. Muzzarelli, G. Biagini, A. DeBenedittis, P. Mengucci, G. Majni, and G. Tosi, *Carbon. Polym.*, **45**, 35 (2001).
(30) P. X. Ma, B. Schloo, D. Mooney, and R. Langer, *J. Biomed. Mater. Res.*, **29**, 1587 (1995).
(31) E. Wintermantel, J. Mayer, J. Blum, K. L. Eckert, P. Luscher, and M. Mathey, *Biomaterials*, **17**, 83 (1996).
(32) E. T. Baran, K. Tuzlakoglu, A. J. Salgado, and R. L. Reis, *J. Mater. Sci., Mater. Med.*, **15**, 161 (2004).
(33) C. Schugens, V. Maquet, C. Gradfils, R. Jerome, and P. Teyssie, *J. Biomed. Mater. Res.*, **30**, 449 (1996).
(34) L. L. Whinnery, W. R. Even, J. V. Beach, and D. A. Loy, *J. Polym Sci., Polym. Chem.*, **34**, 1623 (1996).
(35) D. K. Kim and H. S. Kim, *Polymer(Korea)*, **29**, 408 (2005).
(36) S. J. Park, K. Y. Lee, W. S. Ha, and S. Y. Park, *J. Appl. Polym. Sci.*, **74**, 2571 (1999).
(37) N. C. Braier and R. A. Jishi, *J. Mol. Struct. (Theochem)*, **499**, 51 (2000).
(38) I. Yamaguchi, S. Itoh, M. Suzuki, A. Osaka, and J. Tanaka, *Biomaterials*, **24**, 3285 (2003).
(39) C. J. Brine, P. A. Sandford, and J. P. Zikakis, *Advances in Chitin and Chitosan*, Elsevier Applied Science, London, 1992.
(40) P. X. Ma and R. Langer, in *Polymers in Medicine and Pharmacy*, Materials Research Society, Pittsburgh, 1995, pp 99-104.
(41) Y. Zhang and M. Zhang, *J. Biomed. Mater. Res.*, **55**, 304 (2001).
(42) N. Shanmugasundaram, P. Ravichandran, P. N. Reddy, N. Ramamurty, S. Pal, and K. P. Rao, *Biomaterials*, **22**, 1943 (2001).
(43) T. J. Webster, C. Ergun, R. H. Doremus, R. W. Siegel, and R. Bizios, *J. Biomed. Mater. Res.*, **51**, 475 (2000).
(44) G. S. Sailaja, S. Velayudhan, M. C. Sunny, K. Sreenivasan, H. K. Varma, and P. Ramesh, *J. Mater. Sci.*, **38**, 3653 (2003).